X. Y. Luo*
Department of Mechanical Engineering
University of Sheffield
Sheffield, S1 3JD, UK

W. G. Li
Hydraulic Machinery Division
Gansu University of Technology
730050, Lanzhou, P.R. China

J. Li
School of Civil Engineering and Mechanics
Xi'an Jiaotong University
710049, Xi'an, P. R. China

Geometrical Stress-Reducing Factors in the Anisotropic Porcine Heart Valves

This study carries out a detailed parameter study based on a nonlinear anisotropic finite-element model published previously. The aim of this study is to identify the stress-reducing influences from geometrical parameters such as stent height, valve diameter, and the nonuniform thickness of porcine aortic valves under static loading condition. The anisotropy of the valve is considered to be transversely isotropic with fibers oriented along the circumferential directions, which enables us to use a simple anisotropic constitutive model using uniaxial experimental data. The results showed that in general, higher stent height and smaller diameter combined with nonuniform thickness give rise to a much more reduced overall stress level. Although the absolute values of the peak stresses may be influenced by the detailed orientations of fibers, the trends of the stress variation with the geometrical factors seem to be qualitatively consistent within the parameter ranges considered. [DOI: 10.1115/1.1614821]

1 Introduction

Prosthetic heart valves have become increasingly used in the treatment of congenital abnormalities and cardiovascular disease since their introduction in the early 1960s. These artificial heart valves may be either tissue or mechanical. Tissue valves offer many advantages over the mechanical alternatives in that they are much more compatible with the patients who do not need long-term anticoagulation. However, their mid- and long-term durability is low, especially in children and young adults [1].

The degeneration is mainly due to calcification and tearing of the valve leaflets. It is widely believed that the stress concentration plays an important role in the degeneration. Consequently, numbers of studies on stress analyses of heart valves have been carried out in the last 20 years. In the earlier years, simpler membrane models of heart valves were used [2–6], but mostly employed non-linear membrane elements, sometimes with truss elements embedded. Later, it was discovered that bending stress in the valve cannot be neglected; subsequently 2-D square elements with bending stiffness [7], as well as 3-D brick elements [8] were employed to model the mechanical behavior of the valves. More recent models have been built with nonlinear shells, and computations were carried out using commercial packages such as Marc, DYNA3D or ANSYS [9–14]. The majority of these numerical studies have assumed that the valves behave in an isotropic fashion. However, it has recently been confirmed that the anisotropy of heart valves plays an important role in the valve stress distributions [15,16].

Native valves, such as porcine and human heart valves, are highly nonlinear and anisotropic. These material properties should be considered when modelling the stress distributions in these valves. Implementation of stress reducing mechanisms found in the natural aortic valve is important for optimal bioprosthetic valve designs. A proper understanding of these stress reducing mechanisms requires one to identify the key parameters which govern the stress distributions in the natural valve. It is for this purpose that the present paper is devoted to a detailed parameter study that takes into account of both nonlinearity and anisotropy of the porcine valves, as well as geometrical variations.

*Corresponding author: Phone: +44 114 2227752; Fax: +44 114 2227890; e-mail: X.Y.Luo@shef.ac.uk.

Contributed by the Bioengineering Division for publication in the JOURNAL OF BIOMECHANICAL ENGINEERING. Manuscript received by the Bioengineering Division October 28, 2002; revision received April 9, 2003. Associate Editor: M. Sacks.

The structure of the paper is organized as follows: the constitutive model is briefly reviewed in Section 2, the finite element methods and parameters are described in Section 3. This is followed by results obtained for different parameters both for isotropic and anisotropic cases. Finally, a discussion is given in Section 5.

2 The Anisotropic Constitutive Model

The highly nonlinear and anisotropic behavior of porcine valves has been observed in many experiments [17–25]. It has been discovered that the structure of the porcine valves can be regarded as an elastic meshwork, reinforced with stiff collagen bundles, showing an arrangement in the circumferential direction [16]. Earlier experimental studies were mostly based on uniaxial tests, although some recent work (e.g. [24,25]) was carried out using biaxial ones.

Assuming that porcine valves behave like a simple composite with transverse isotropy, Li et al. [16] showed that five elastic moduli, namely E_x, E_y, ν_x, ν_y, G, for a transversely isotropic composite can be reduced to the following simpler form:

$$E_x = E_x(\varepsilon_x); \quad E_y = E_y(\bar{\varepsilon}) \tag{1}$$

$$G_{xy} = \frac{E_y}{2(1+\nu_{xy})} \tag{2}$$

where x is the local coordinate representing the circumferencial direction of the valve leaflet, y is the radial direction, and $\bar{\varepsilon}$ is the effective strain. The Poisson ratios, ν_{xy}, ν_{yz}, are both chosen to be 0.45 to enforce the (nearly) incompressible property of the soft tissue.

The basic idea behind the model is that if the matrix and the collagen bear the same strain (ε_x) in the circumferential direction, then the contribution to the total stiffness in this direction will be primarily due to collagens (since $E_x \gg E_y$); while in the other direction, both contributions are significant (hence the use of the effective strain, $\bar{\varepsilon}$).

Using this approach, it is possible to make use of the uniaxial experimental data to determine the stress-strain relation, Eq. (1). In this paper, experimental data from Mavrilas and Missirlis [17] is used. For details, see [16].

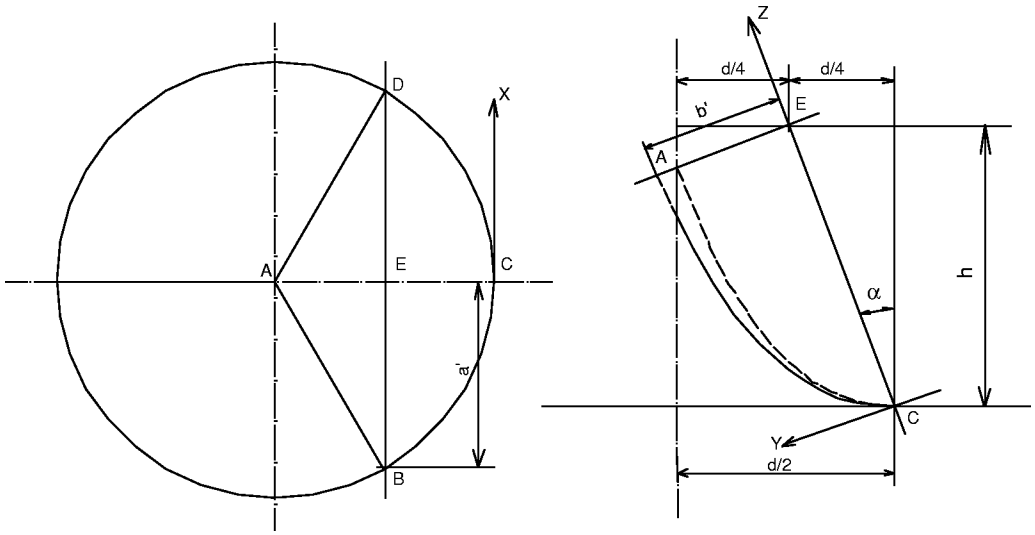

Fig. 1 The top view (left) and the side view (right) of the porcine valve leaflet. The leaflet takes the form of an elliptic paraboloid.

3 The Finite-Element Model and Methods

3.1 The Geometry. Following Hamid et al. [5] we assume that the geometry of the valve in closed and unloaded phase can be described by the elliptic paraboloid equation:

$$\frac{x^2}{a^2}+\frac{y^2}{b^2}=z, \tag{3}$$

where a, b are related to the stent height h and the valve diameter d by:

$$a=\frac{\sqrt{3}d}{4\sqrt{h'}}, \quad b=\frac{d}{4\cos\alpha\sqrt{h'}}$$

$$\alpha=tg^{-1}\left(\frac{d}{4h}\right), \tag{4}$$

$$a'=a\sqrt{h/\cos\alpha}, \quad b'=1.24b\sqrt{h/\cos\alpha}.$$

This geometry is shown in Fig. 1. Using Eq. (4), the area for the whole valve leaflet can be estimated. For $D=27.8$ mm, and $h=19$ mm, the area is about 4.89 cm^2.

3.2 The Finite-Element Model. The finite-element model based on the valve's transverse isotropy is sketched in Fig. 2. The fiber orientations in Fig. 2a are chosen in such a way so that more fiber bundles are allocated near the commissural area, as observed by Sauren et al. [26]. Due to symmetry, only half of the leaflet is computed, see Fig. 2b.

For a rigid stent, the boundary conditions are such that the displacement is zero along the line BC (stent). The condition of zero rotation along the stent is not imposed in this study since in reality the valves are sewn to the stent so that a clamped condition is considered too restrictive. Symmetrical conditions are applied on the midline AC. For the free edge, AB, an incline restraint condition is imposed to mimic a simplified contact condition [16].

The nonlinear stress strain relation is then:

$$\{\Delta\sigma\}=[D(E(\varepsilon)]\{\Delta\varepsilon\}, \tag{5}$$

where $\Delta\sigma$, $\Delta\varepsilon$ are the incremental stress and strain tensors, $[D(E)]$ is the stiffness matrix of the material which depends on the five elastic moduli denoted by E. The final global finite-element matrix equation can be written as:

$$[K]\{U\}=\{F\}, \tag{6}$$

where $[K]$ is the stiffness matrix, $\{U\}$ is the displacement vector, and $\{F\}$ is the load vector. This matrix equation is solved using the update Lagrangian method combined with the modified Newton-Raphson method [16].

The finite element code has been validated carefully in the previous study. It was found that 900 Reisser-Minlin 8-node shell elements with 2921 nodes are sufficient for the computational accuracy required [16].

3.3 The Parameters. A systolic pressure of P=16 kPa (120 mmHg) is applied to the closed valve in a static phase. The main parameters in a stented porcine aortic valve are the stent height and the valve diameter. The diameters are chosen to be within the range of the stented bioprosthetic aortic valves made by AORTECH (AORTECH International PLC). For a given diameter, a range of different stent heights can be used. The parameter ranges studied in this paper are listed in Table 1. Note that the increment value for the stent height within each range is chosen to be 1 mm.

Most of the numerical simulations published to date have assumed uniform thickness for the valve leaflet. However, porcine heart valves exhibit extensive variation in thickness from 0.2 mm in the belly zone to 1.4 mm to the free edge [27] as shown in Fig. 3. In this paper, non-uniform thickness is also considered as a parameter. For comparison, the corresponding nonlinear isotropic

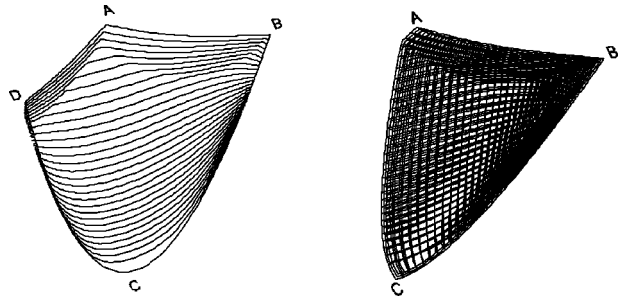

Fig. 2 (left) The fibre orientations and (right) the finite element model (only half of the leaflet is computed) with 900 nodes. As three nodes are used along the shell thickness, there are three layers in the finite element model.

Table 1 The parameters of the stented porcine aortic valves

Diameter, d (mm)	Stent height, h (mm)	Isotropic	Anisotropic	Uniform thickness (mm)	Nonuniform thickness (mm)
20	14–29	Yes	Yes		
24	13–24	Yes	Yes	0.6	0.2–1.4
27.8	12–20	Yes	Yes		

model is also computed for all parameters. The stress-strain curve for the isotropic model is taken to be the average of the two stress-strain curves in the circumferential and radial directions, as shown in Fig. 4.

4 Results

4.1 Stress Distributions for Valves of Uniform Thickness. The distributions of the longitudinal normal stress (in the circumferential direction), the transverse normal stress (in the radial direction), and the in-plane shear stress for both isotropic and anisotropic porcine valves with a uniform thickness are shown in Fig. 5, for $d=27.8$ mm, and h=19 mm.

It is notable that the longitudinal normal stress is the most significant stress component present in the valve. This is because the longitudinal normal stress is very close to the first principal stress (in the composite mechanics, however, the term first principal stress is less commonly used). It is not surprising to see that the longitudinal normal stress level increases in the anisotropic case. The stress concentration occurs at the area where the fibers are more compactly located. Consequently, the other two stress components, namely, transverse normal and in-plane shear stresses are reduced in this case. However, the difference, in terms of magnitude, between the isotropic and anisotropic cases for these two stress components is not as significant as in longitudinal normal stress.

The distributions of the longitudinal normal stress for different stent heights and $d=27.8$ mm are shown in Fig. 6. There are a few observations to be made on this figure. Firstly, for the isotropic valves, the peak longitudinal normal stress seems to appear always at the top of the stent height, while for anisotropic ones it is

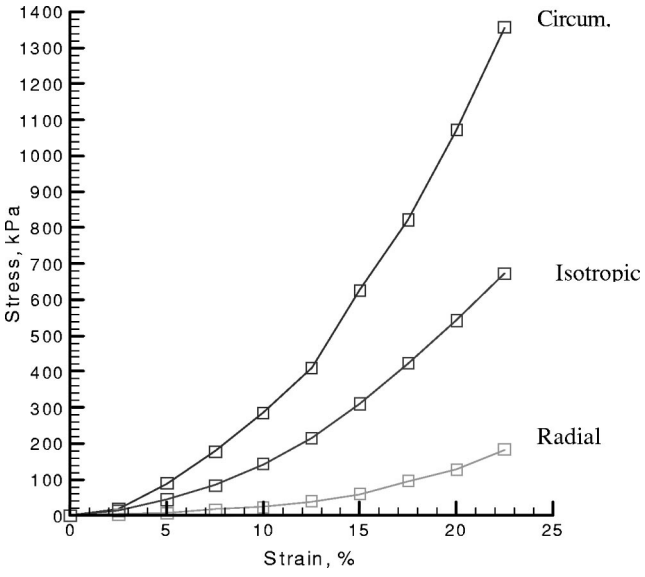

Fig. 3 Representative stress-strain curves in the circumferential and radial directions for fresh porcine valve measured by Mavrilas & Missirlis [17]. The stress-strain curve for the corresponding isotropic model is taken as the average of the two curves, as shown in the middle.

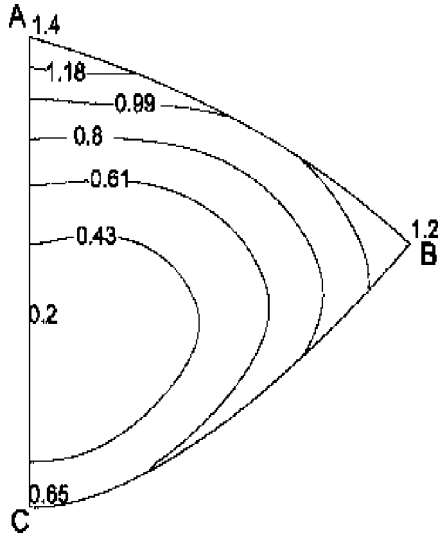

Fig. 4 The variation in thickness of the porcine valves. The thickness counters are based on the measurements by Clark & Finke [27].

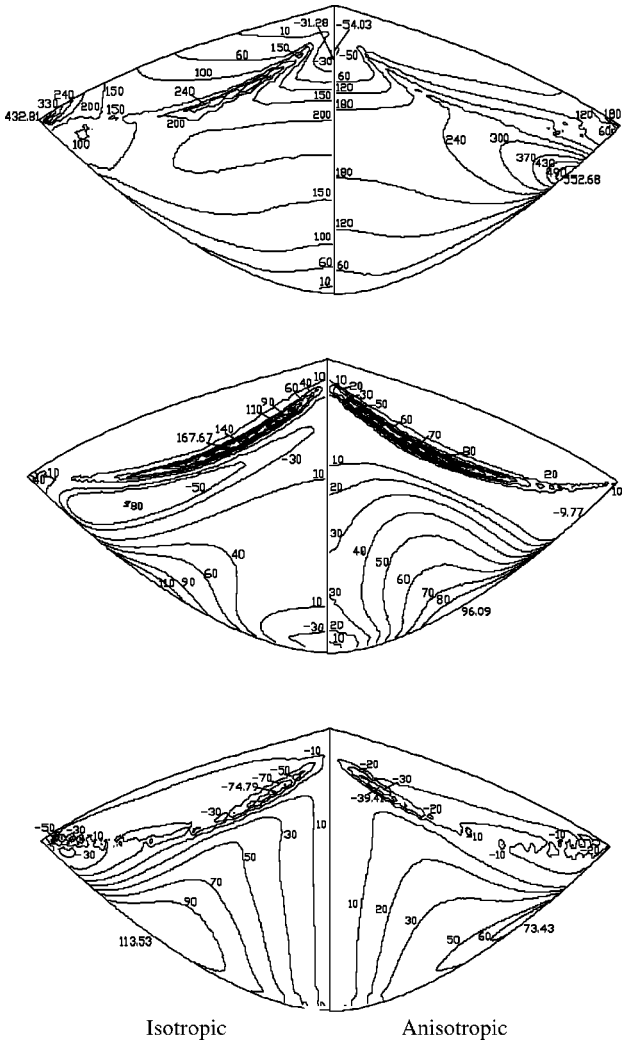

Fig. 5 The stress contours for porcine valves with a uniform thickness. Top: longitudinal normal stress; middle: transverse normal stress; and bottom: in-plane shear stress. $d=27.8$ mm, h=19 mm. The values on the contours are given in kPa.

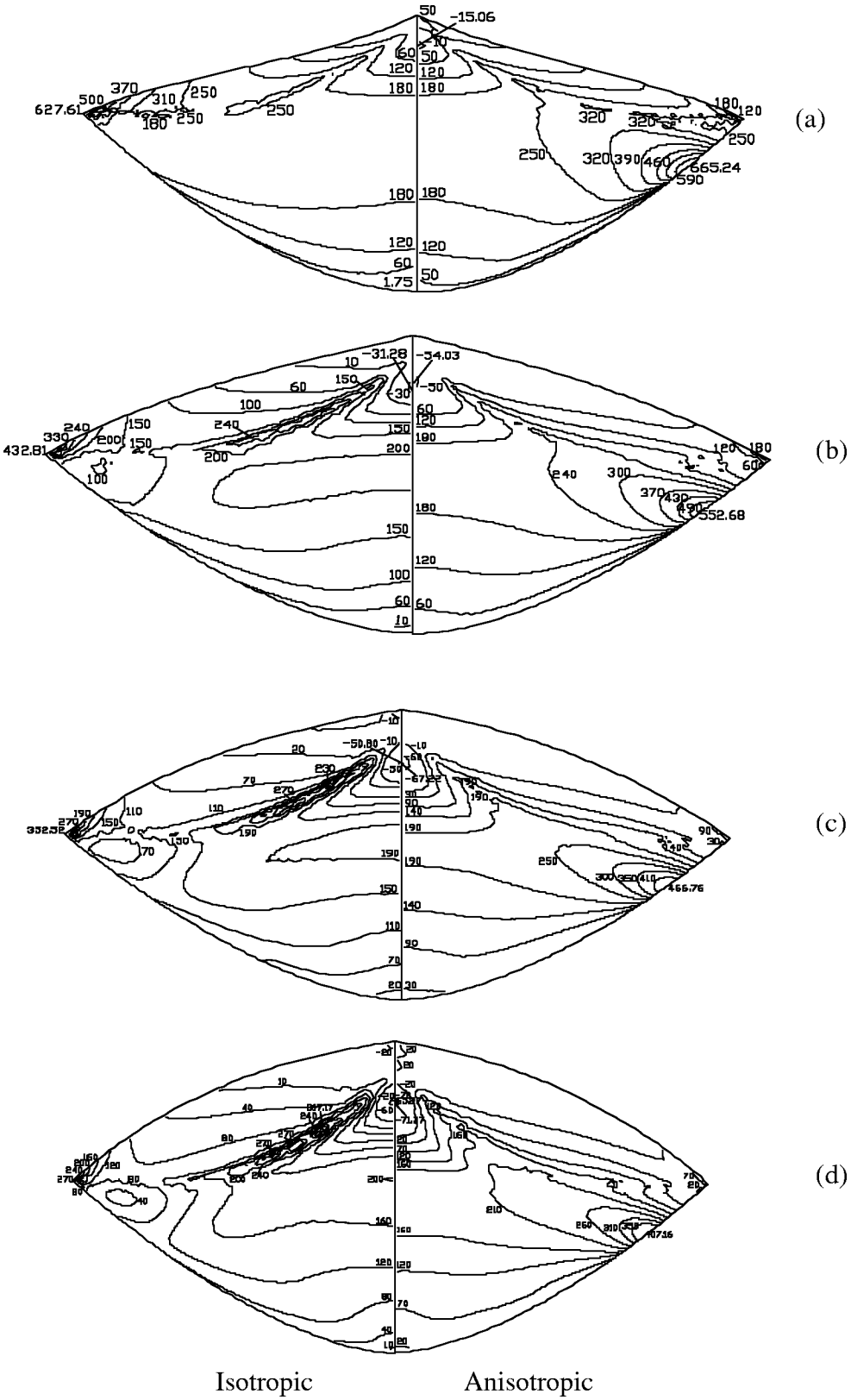

Fig. 6 The longitudinal normal stress contours on the top surface of a porcine valves with uniform thickness for $d=27.8$ mm, and (a) $h=14$ mm, (b) $h=19$ mm, (c) $h=24$ mm, and (d) $h=28$ mm. The values on the contours are given in kPa.

shifted slightly below. This happens consistently in all the geometries, and is obviously due to the fact that the fibers are packed much more densely near the commissural area, as reported by Sauren et al. [26]. Secondly, the stress concentration at the contact area seems to be less severe in the anisotropic cases. Finally, the value of the peak longitudinal normal stress decreases as the stent height is increased, and this happens both for isotropic and anisotropic cases.

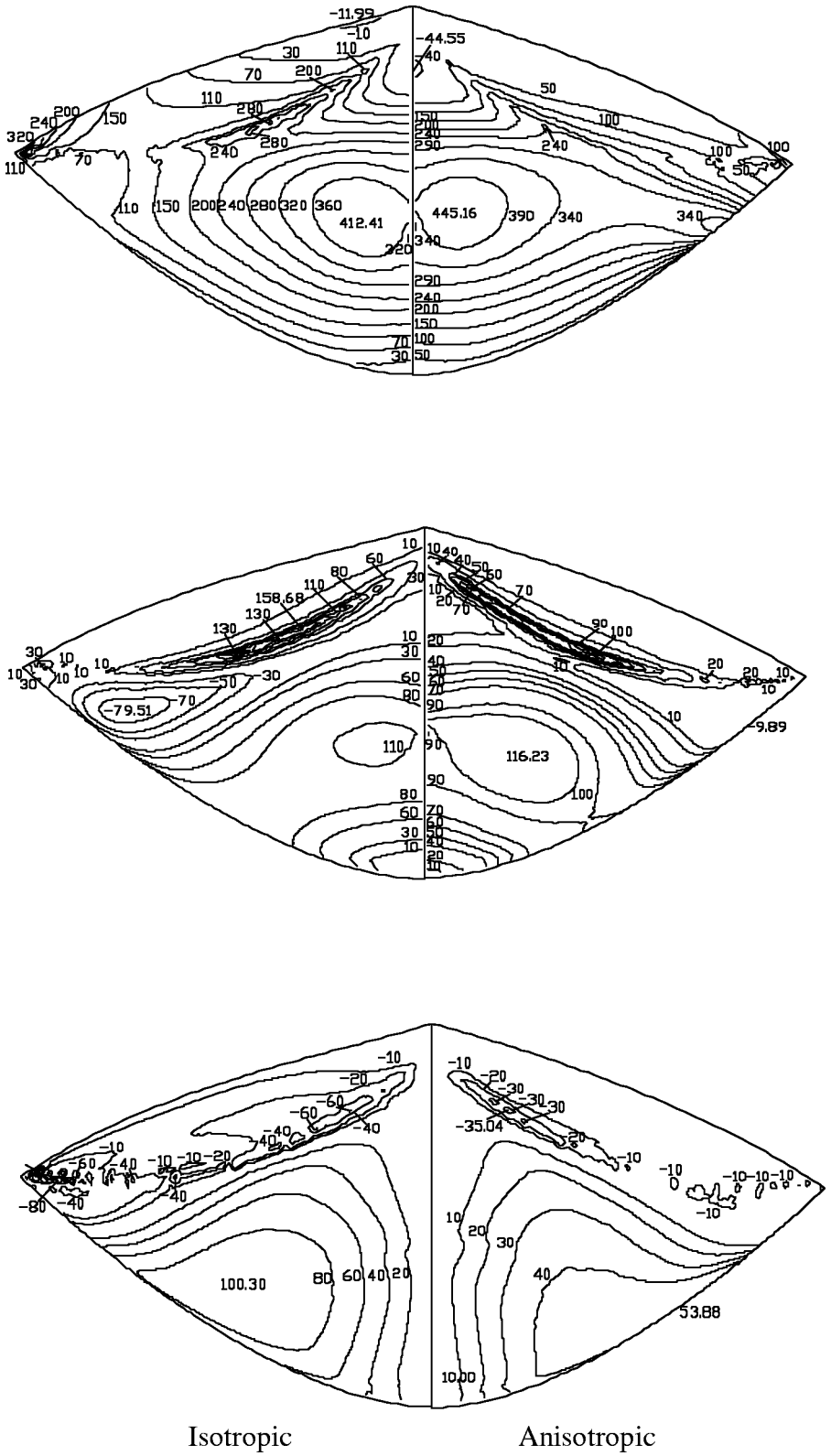

Fig. 7 The stress contours for porcine valves with a non-uniform thickness. Top: longitudinal normal stress; middle: transverse normal stress; and bottom: in-plane shear stress. $d=27.8$ mm, $h=19$ mm. The values on the contours are given in kPa.

4.2 Stress Distributions for Valves of Nonuniform Thickness. The longitudinal normal, transverse normal and in-plane shear stress distributions for the valve leaflet of nonuniform thickness are shown in Fig. 7 for $d=27.8$ mm, $h=19$ mm. This is to be compared with Fig. 5. The longitudinal normal stress contours for different stent heights and $d=27.8$ mm are also shown in Fig. 8, to be compared with Fig. 6.

On the whole, the stress patterns seem to be much more evenly

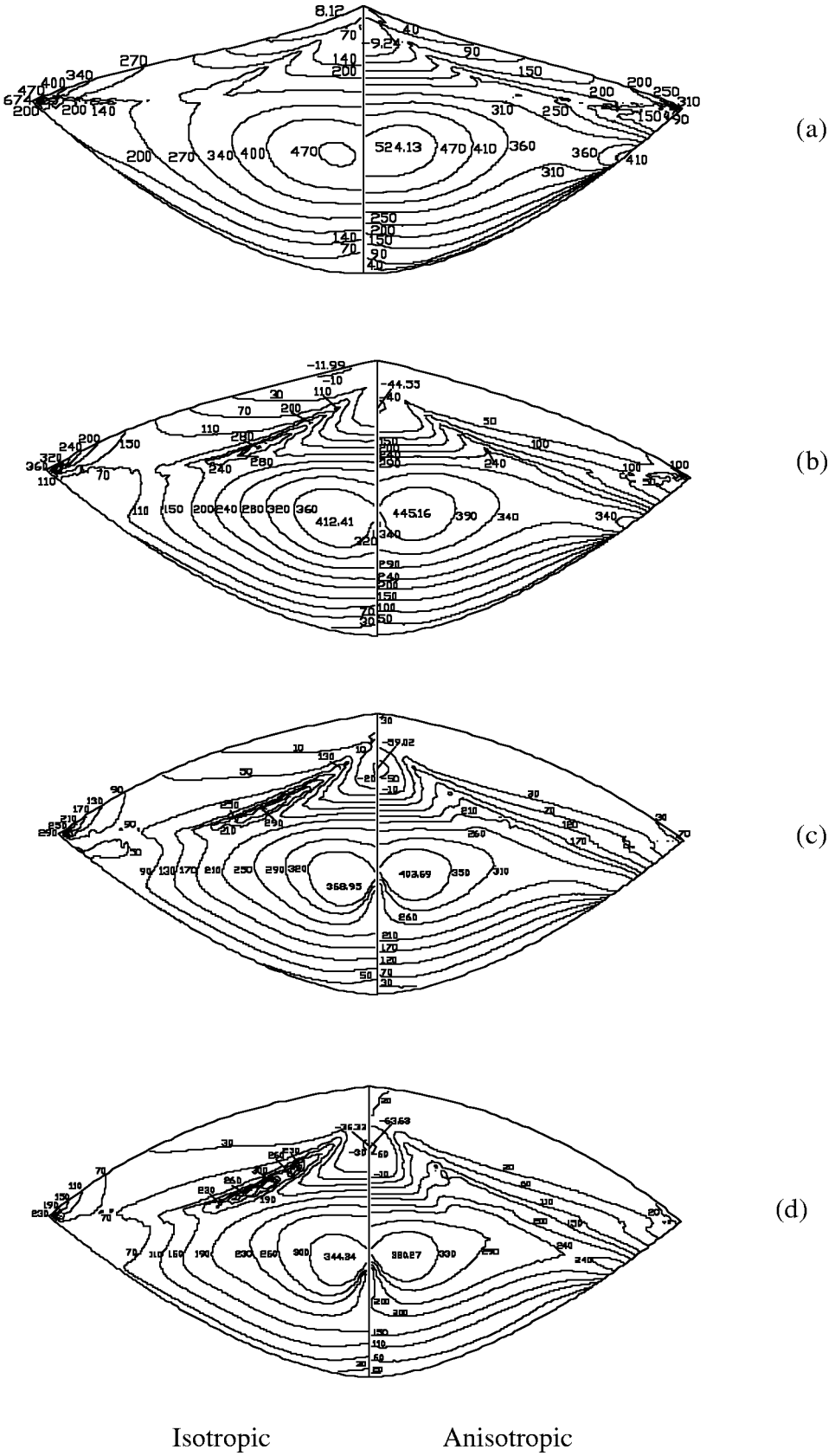

Fig. 8 The longitudinal normal stress contours on the top-surface of a porcine valve with the nonuniform thickness, and for $d=27.8$ mm, and (a) $h=14$ mm, (b) 19 mm, (c) 24 mm, and (d) 28 mm. The values on the contours are given in kPa.

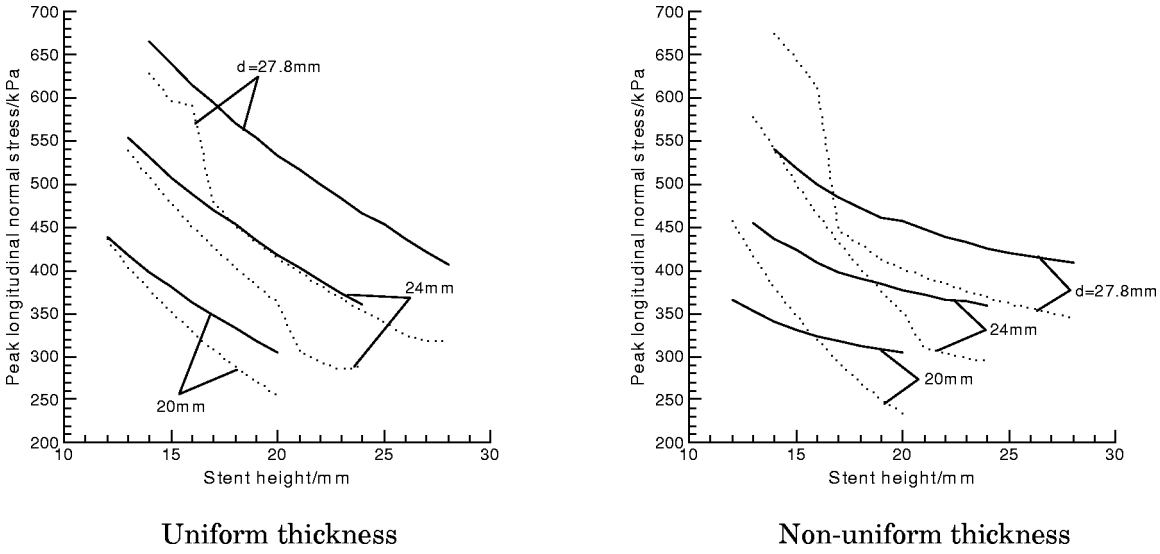

Fig. 9 The peak longitudinal normal stress versus the stent height for porcine valves with three different diameters. The solid curves are results from the anisotropic valves, and the dashed ones are for the corresponding isotropic valves.

distributed in the nonuniform thickness cases, suggesting that the non-uniform thickness acts as a stress reducing mechanism. One important difference from the results in Section 4.1 is that for both isotropic and anisotropic cases, a secondary stress concentration occurs in the belly zone. This is because the belly zone is much thinner than the rest of the leaflet. Therefore, for the same loading condition, it yields a larger deformation, and hence a greater stress.

It is noted, however, that the original high-stress sites for valves of uniform thickness (see Section 4.1) remain unchanged, i.e., the peak longitudinal normal stress stays at the stent top for the isotropic case, and at the commissural area just below the top for the anisotropic case. The nonuniform thickness seems to only reduce the intensity of these stress concentrations.

4.3 The Peak Stress Variations With Diameter and Stent Height. The variation of the peak stresses with different geometries can be investigated in more detail here. The peak longitudinal normal stress versus stent height for three different diameters is plotted in Fig. 9, for both uniform and nonuniform thickness. The dashed curves in Fig. 9 are for the isotropic model, and the solid ones are for the anisotropic model. For all cases, the peak longitudinal normal stress *decreases* with the stent height. Also, a *smaller* diameter seems to correspond to a much lower stress level. Again as we observed in Section 4.2, the nonuniform thickness of the valve gives rise to a much reduced stress pattern. This is even more significant in the nonuniform thickness case.

The variation of the peak transverse normal stress with the stent height and valve diameter is shown in Fig. 10. In contrast to the longitudinal normal stress, the general peak transverse normal stress level is much lower in the anisotropic case. In addition, the nonuniform thickness seems to decrease the peak transverse stress only in the isotropic case; the peak stress is increased by a small amount due the nonuniform thickness in the anisotropic case. On the other hand, a lower transverse stress level still corresponds to

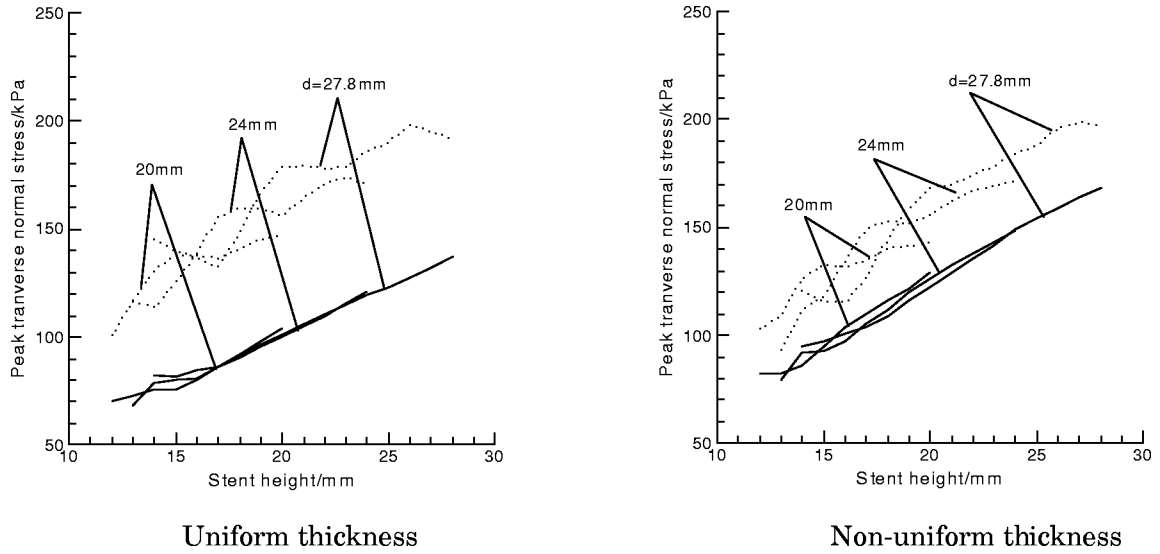

Fig. 10 The peak transverse normal stress versus the stent height for porcine valves with three different diameters. The solid curves are results from the anisotropic valves, and the dashed ones are for the corresponding isotropic valves.

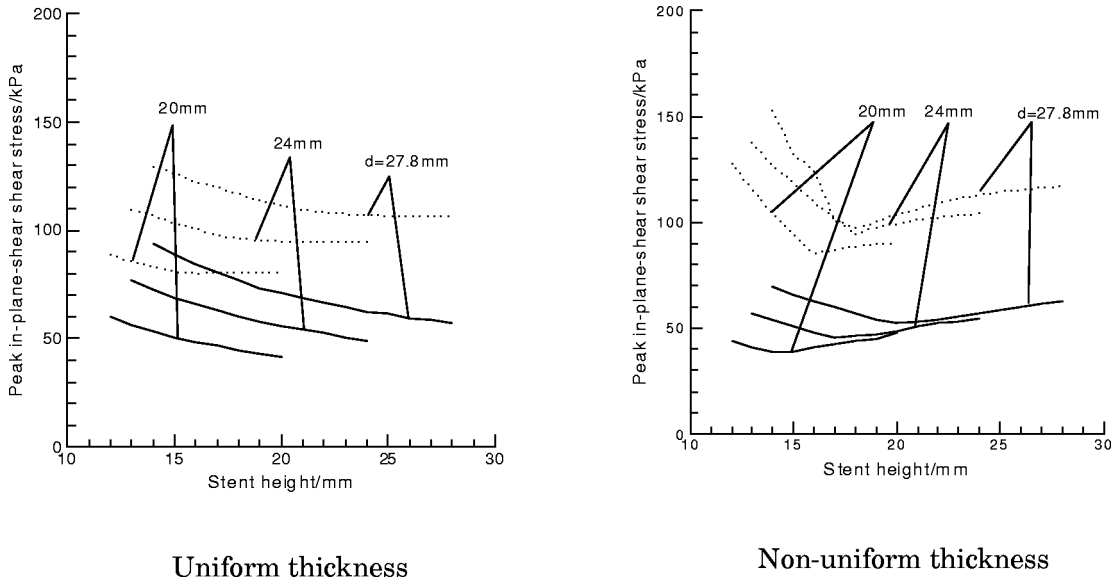

Fig. 11 The peak in-plane shear stress versus the stent height for porcine valves with three different diameters. The solid curves are results from the anisotropic valves, and the dashed ones are for the corresponding isotropic valves.

a higher stent height for both isotropic and anisotropic cases, while the diameter seems to have very little effect on the peak transverse stress.

Variation of the peak in-plane shear stress with the stent height and valve diameter is shown in Fig. 11. The anisotropy also reduces the peak in-plane shear stress, for both uniform and nonuniform thickness cases. The peak in-plane shear seems to decrease slightly with stent height for the uniform thickness, but this trend is not clearly present in the nonuniform case. It is again noticeable that the smaller diameter gives rise to a lower level of the peak stress, but the nonuniform thickness seems to have very little effect here.

5 Discussion

This paper assesses the geometrical factors that may reduce the stress concentrations in porcine valves using an anisotropic model published previously [16]. A composite constitutive model is used whereby the elastic moduli were estimated from uniaxial experimental data. It could be argued that biaxial experimental data are more suitable in constructing the constitutive model. However, very few biaxial experimental data reported to date are complete enough to construct a universal constitutive model [18], Billiar and Sacks [24,25] have reported a more complicated constitutive model based on their biaxial measurements of porcine aortic valves, but their model is derived for a thin membrane, not a shell of finite thickness used here. In addition, if the valve structure is truly transversely isotropic, as we have assumed, then the coupling effect from the radial to the circumferential direction (which is absent in our model) is less significant, since the ratio of the elastic moduli between the two directions is large (>6).

We have seen that detailed fiber orientations can be important. In the anisotropic case, the area packed with more fibers gives rise to high stress concentrations. The fiber orientations we assumed in this paper are chosen to be similar to that observed by Sauren et al. [26]. To see if our results are robust for small changes of the fiber orientations, we have changed the fiber orientations slightly, and discovered that, although the absolute values of the peak stresses may be different, the trends of the peak stresses with the stent height and valve diameter as shown in Figs. 9–11 are similar. This observation is supported by the fact that even in the extreme (isotropic) case where no fibers are present, the peak stresses still present some similar variations with the stent height and valve diameters in Figs. 9–11. Therefore, we believe our observations are useful as a general design guide for bioprosthetic heart valves. However, if the absolute values of the stresses in the valves are of a major concern, then the elastic moduli of this constitutive model should be estimated from more precisely measured fiber orientations and perhaps constructed from biaxial or even 3-D experiments.

In all the results showed above, the commissure edge and belly zone are found to be the most vulnerable sites for a valve with non-uniform thickness and anisotropy. These two sites are directly associated with the areas of more compact fiber bundles or with regions where the valves are thinner. This is in agreement with the experimental study by Milano et al. [28], in which they found that 98% of calcific deposits were located near the commissural area and 76% were in the body of cusps.

It should be noted that unlike Hamid's calculations [5] where a constant leaflet area is used throughout, we did not fix the area of the paraboloidal leaflet in our calculations. Therefore, the area can change with the different geometric parameters used. The area variation with the stent height and the valve diameter is shown in Fig. 12. In Fig. 12, the area increases both with the stent height and diameters, as expected. One might at first speculate that the decrease of the longitudinal normal stress with the stent height found in our simulations is simply due to the corresponding increase of the valve area. However, if this is true, then the decrease of the stress with the diameter would be difficult to explain. In addition, this stress decrease with the stent height has also been observed by Hamid et al. [5] for isotropic and uniform thickness valves with a fixed valve area.

We believe the most important geometrical influence on the stress distributions is associated with the way the valves facing the systolic pressure. For a greater stent height, or a smaller diameter, the valve tends to curve away more from the direction of the pressure, therefore reducing the longitudinal normal stress. This can also explain the increase of the transverse normal stress, as this configuration induces extra stretch in the radial direction. This seems to strongly suggest that to reduce the longitudinal normal stress in the valve, the stent height should be increased, or the diameter decreased. However, one should be cautious here as it has also been argued that a smaller stent height would minimize protrusion of the struts into the left ventricular outflow tract into the aorta and may also reduce turbulence [29].

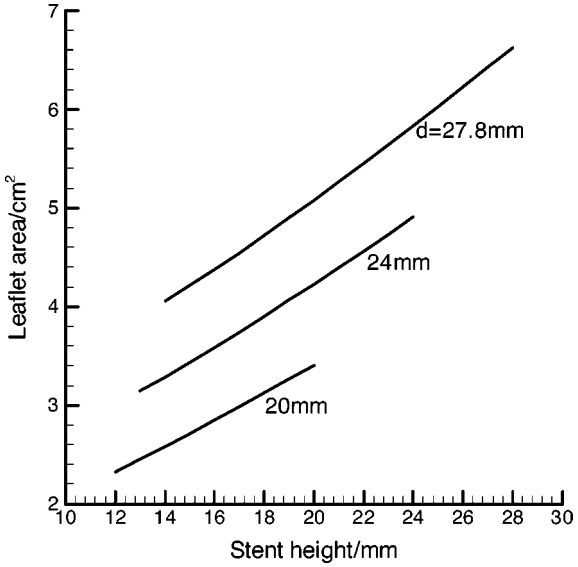

Fig. 12 The variation of the area of the valve with the stent height for the three different diameters used

Limitations. There are several limitations in the results from this study. First, only static loading is considered, whereas the dynamic behavior of the valves can be important. Three-dimensional dynamic simulations of bioprosthetic aortic valves have been performed before [15,30]. However, as time dependent stress analysis involves highly complicated blood flows as well as fluid and structure interactions, it is as yet beyond our computational power to carry out an extensive parameter study, as we have done here, for anisotropic valves under a dynamic loading. In addition, although the valve undergoes a dynamic pressure and stresses during the cycling phase, it experiences its maximum stress level when it is closed.

Other limitations of the work are that the valve is assumed to be symmetric, with the leaflet shape prescribed by an elliptic paraboloid, and the contact area described by a simpler incline constraint. Actual 3-D geometries have been considered previously [30]. However, as these geometries are subject dependent, the ''irregularity'' of the geometry cannot be easily incorporated into a parameter study without losing its generality. Also, as mentioned before, due to the lack of sufficient experimental data, at the present the elastic moduli from this model are still estimated from uniaxial studies.

6 Conclusion

A detailed parameter study of finite element simulations is carried out to analyze the stress distribution for a nonlinear and anisotropic porcine heart valve. The results are compared with the corresponding isotropic porcine valves for both uniform and non-uniform valve thickness. This is the first time that these geometrical effects are assessed in detail for non-linear and anisotropic porcine valves.

It is found that the anisotropy tends to move the stress concentrations towards the area of more densely packed fibers. Consequently, the peak longitudinal normal stress increases, and the peak transverse normal and in-plane shear stresses decrease. Non-uniform thickness plays a significant role in reducing all the peak normal stresses, as a result of much more evenly distributed stress patterns. This is true for both anisotropic and isotropic cases.

Higher stent height reduces the longitudinal normal stress, and increases the transverse normal stress, but has no obvious effect on the in-plane shear stress. Therefore, if the longitudinal normal and in-plain shear stresses concentration are of concern, then it would be advantageous to use the highest allowed stent height. Finally, it has been discovered that the smaller the diameter, the better the stress distributions in the valve leaflets in all cases.

Acknowledgment

This work is supported by the Royal Society of London.

References

[1] Jamieson, W. R. E., Burr, L. H., Munro, A. I., and Miyagishima, R. T., 1998, ''Carpenter-Edwards Standard Porcine Bioprosthesis: A 21-Year Experience,'' Ann. Thorac. Surg., **66**, pp. S40–43.
[2] Ghista, D. N., and Reul, H., 1977, ''Optimal Prosthetic Aortic Leaflet Valve; Design Parametric and Longevity Analysis: Development of the Avcothane-51 Leaflet Valve Based on the Optimal Design Analysis,'' J. Biomech., **10**, pp. 313–324.
[3] Christine, C. W., and Medland, I. C., 1982, ''A Nonlinear Finite-Element Stress Analysis of Bioprosthetic Heart Valve,'' In: *Finite Element in Biomechanics*, Gallagher, R. H., Simon, B. R., Johnson, P. C., and Gross, J. F. eds., Chichester, Wiley, pp. 153–179.
[4] Hamid, M. S., Sabbah, H. N., and Stein, P. D., 1985, ''Finite-Element Evaluation of Stresses on Closed Leaflets of Bioprosthetic Heart Valves With Flexible Stent,'' Finite Elem. Anal. Design, **1**, pp. 213–225.
[5] Hamid, M. S., Sabbah, H. N., and Stein, P. D., 1986, ''Influence of Stent Height Upon Stresses on the Cusps of Closed Bioprosthetic Valves,'' J. Biomech., **19**, pp. 759–769.
[6] Rousseau, E. P. M., Sauren, A. A. H. J., van Hout, M. C., and van Steenhoven, A. A., 1983, ''Elastic and Viscoelastic Material Behavior of Fresh and Glutaraldehyde-Treated Porcine Aortic Valve Tissue,'' J. Biomech., **16**, pp. 339–348.
[7] Huang, X., Black, M. M., Howard, I. C., and Patterson, E. A., 1990, ''Two-Dimensional Finite-Element Analysis of a Bioprosthetic Heart Valve,'' J. Biomech., **23**, pp. 753–762.
[8] Krucinski, S., Vesely, I., and Dokainish, M. A., 1993, ''Numerical Simulation of Leaflet Flexure in Bioprosthetic Heart Valves Mounted on Rigid and Expansible Stents,'' J. Biomech., **26**, pp. 929–943.
[9] Black, M. M., Howard, I. C., Huang, X., and Patterson, E. A., 1991, ''Three-Dimensional Finite Element Analysis of a Bioprosthetic Heart Valve,'' J. Biomech., **24**, pp. 793–801.
[10] Patterson, E. A., Howard, I. C., and Thornton, M. A., 1996, ''A Comparative Study of Linear and Nonlinear Simulations of the Leaflets in a Bioprosthetic Heart Valve During Cardiac Cycle,'' J. of Medical Engineering and Technology, **20**, pp. 95–108.
[11] Thornton, M. A., Howard, L. C., and Patterson, E. A., 1997, ''Three-Dimensional Stress Analysis of Polypropylene Leaflets for Prosthetic Heart Valves,'' Med. Eng. Phys., **19**, pp. 588–597.
[12] Grande, K. J., Cochran, R. P., Reinhall, P. G., and Kunzelman, K. S., 1998, ''Stress Variations in the Human Aortic Root and Valve: The Role of Anatomic Asymmetry,'' Ann. Biomed. Eng., **26**, pp. 534–545.
[13] Grande, K. J., Cochran, R. P., Reinhall, P. G., and Kunzelman, K. S., 1999, ''Mechanisms of Aortic Root and Valve Incompetence in Aging: A Finite-Element Model,'' J. Heart Valve Dis., **8**, pp. 149–159.
[14] De Hart, J., Cacciola, G., Schreurs, P. J. G., and Peters, G. W. M., 1998, ''A Three-Dimensional Analysis of a Fiber-Reinforced Aortic Valve Prosthetics,'' J. Biomech., **31**, pp. 629–638.
[15] Burriesci, G., Howard, I. C., and Patterson, E. A., 1999, ''The Stress/Strain and Fatigue Behavior of Glutaraldehyde Preserved Heart-Valve Tissue,'' J. Biomech., **10**, pp. 707–724.
[16] Li, J., Luo, X. Y., and Kuang, Z. B., 2001, ''A Nonlnear Anisotropic Model for Porcine Aortic Heart Valves,'' J. Biomech., **34**, pp. 1279–1289.
[17] Mavrilas, D., and Missirlis, Y., 1991, ''An Approach to the Optimization of Preparation of Bioprosthetic Heart Valves,'' J. Biomech., **24**, pp. 331–339.
[18] Mayne, A. S. D., Christie, G. M., Smaill, B. H., Hunter, P. J., and Barratt-Boyes, B. G., 1989, ''An Assessment of the Mechanical Properties of Leaflets From Four Second-Generation Porcine Bioprosthese With Biaxial Testing Techniques,'' J. Thorac. Cardiovasc. Surg., **98**, pp. 170–180.
[19] Vesely, I., 1998, ''The Role of Elastin in Aortic Valve Mechanics,'' J. Biomech., **31**, pp. 115–123.
[20] Vesely, I., and Noseworthy, R., 1992, ''Micromechanics of the Fibrosa and the Ventricularis in Aortic Valve Leaflets,'' J. Biomech., **25**, pp. 101–113.
[21] Vesely, I., and Lozon, A., 1993, ''Natural Preload of Aortic Valve Leaflet Components During Glutaraldehyde Fixation: Effects on Tissue Mechanics,'' J. Biomech., **26**, pp. 121–131.
[22] Vesely, I., Boughner, D. R., and Leesondietrich, J., 1995, ''Bioprosthetic Valve Tissue Viscoelasticity-Implications on Accelerated Pulse Duplicator Testing,'' Ann. Thorac. Surg., **60**, pp. S379.
[23] Purinya, B., and Kasyanov, V., 1994, ''Biomechanical and Structural Properties of the Explanted Bioprosthetic Valve Leaflets,'' J. Biomech., **27**, pp. 1–11.
[24] Billiar, K. L., and Sacks, M. S., 2000a, ''Biaxial Mechanical Properties of the Native and Glutaraldehyde Treated Aortic Valve Cusp: Part I-Experimental Results,'' ASME J. Biomech. Eng., **122**, pp. 23–30.
[25] Billiar, K. L., and Sacks, M. S., 2000b, ''Biaxial Mechanical Properties of the Native and Glutaraldehyde Treated Aortic Valve Cusp: Part II-A Structural Constitutive Model,'' ASME J. Biomech. Eng., **122**, pp. 327–335.
[26] Sauran, A. A. H., Kuijpers, W., van Steenhoven, A. A., and Veldpaus, F. E.,

1980, ''Aortic Valve Histology and Its Relation With Mechanics-Preliminary Report,'' J. Biomech., **13**, pp. 97–104.
[27] Clark, R. E., and Finke, E. H., 1974, ''Scanning and Light Microscopy of Human Aortic Leaflets in Stressed and Relaxed States,'' J. Thorac. Cardiovasc. Surg., **67**, pp. 792–803.
[28] Milano, A., Bortolotti, U., Talenti, E., Valfre, C., Arbustini, E., Valente, M., Mazzucco, A., Gallucci, V., and Thiene, G., 1984, ''Calcific Degeneration as the Main Cause of Procine Bioprothetic Valve Faiture,'' Am. J. Cardiol., **53**, pp. 1066–1070.
[29] Carpentier, A., Dubost, C., Lane, E., Nashef, A., Carpentier, S., Relland, J., Deloche, A., Fabiani, J. N., Chauvaud, S., and Chauvaud, S., 1982, ''Continuing Improvements in Valvular Bioprostheses,'' J. Thorac. Cardiovasc. Surg., **83**, pp. 27–42.
[30] Makhijani, V. B., Yang, H. Q., Dionne, P. J., and Thubrikar, M. J., 1997, ''Three-Dimensional Coupled Fluid-Structure Simulation of Pericardical Bioprosthetic Aortic Valve Function,'' Peric. Aortic Valve Simulation, **43**, pp. M387–392.